1-2011

Kinetic Solution of the Structure of a Shock Wave in a Nonreactive Gas Mixture

Eswar Josyula
Air Force Research Laboratory

Prakash Vedula
Ohio Aerospace Institute, AFRL

William F. Bailey
Air Force Institute of Technology

Casmir J. Suchyta III
Ohio Aerospace Institute, AFRL

Recommended Citation

Eswar Josyula, Prakash Vedula, William F. Bailey, Casimir J. Suchyta; Kinetic solution of the structure of a shock wave in a nonreactive gas mixture. Physics of Fluids 1 January 2011; 23 (1): 017101. https://doi.org/10.1063/1.3541815

RESEARCH ARTICLE | JANUARY 25 2011

Kinetic solution of the structure of a shock wave in a nonreactive gas mixture

Eswar Josyula; Prakash Vedula; William F. Bailey; Casimir J. Suchyta, III

Physics of Fluids 23, 017101 (2011)
https://doi.org/10.1063/1.3541815

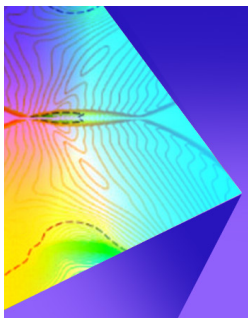

Kinetic solution of the structure of a shock wave in a nonreactive gas mixture

Eswar Josyula,[1] Prakash Vedula,[2,a)] William F. Bailey,[3] and Casimir J. Suchyta III[2]
[1]*Air Force Research Laboratory, Wright–Patterson AFB, Ohio 45433-7512, USA*
[2]*Ohio Aerospace Institute, AFRL/RBAT, Wright-Patterson AFB, Ohio 45433–7512, USA*
[3]*Department of Physics, Air Force Institute of Technology, Wright–Patterson AFB, Ohio 45433–7765, USA*

(Received 7 June 2010; accepted 10 December 2010; published online 25 January 2011)

The multispecies Boltzmann equation is numerically integrated to characterize the internal structure of a Mach 3 shock wave in a hard sphere gas. The collision integral is evaluated by the conservative discrete ordinate method [F. G. Tcheremissine, Comput. Math. Math. Phys. **46**, 315 (2006)]. There was excellent agreement of macroscopic variables [Kosuge *et al.*., Eur. J. Mech. B/Fluids **20**, 87 (2001)]. The effect of species concentration and mass ratio on the behavior of macroscopic variables and distribution functions in the structure of the shock wave is considered for both two- and three-species gas mixtures. In a binary mixture of gases with different masses and varying concentrations, the temperature overshoot of the parallel component of temperature near the center of the shock wave is highest for the heavy component when the concentration of the heavy component is the smallest. The rise in the parallel component of temperature is revealed by the behavior of the distribution function. [doi:10.1063/1.3541815]

I. INTRODUCTION

There is considerable challenge in the design of aerospace vehicles flying at high altitude in the transitional flow region.[1] The strong shock wave around the high speed vehicle redistributes the kinetic energy of the oncoming flow into the translational and internal energy modes, which relax relatively slowly, leading to significant chemical and thermal nonequilibria in the stagnation region. In the gas kinetic description, intermolecular collisions change the translational, rotational, vibrational, and electronic energies of the collision partners. The probabilities or effective cross sections of these elementary processes differ significantly, giving rise to widely separated relaxation times for the internal modes. Thus it becomes important to account for the rates of relaxation to predict the nonequilibrium behavior of these flows. Equilibrium is established relatively fast for the translational degree of freedom compared to internal degrees of freedom. The equilibrium Maxwellian distribution is established as a result of the exchange of momentum and kinetic energy among particles. The relaxation time (τ_{trans}) for establishing a Maxwellian distribution in the components of air is of the order of the average time (τ_{gas}) between collisions, $\tau_{\text{trans}} \approx \tau_{\text{gas}} = (l/v) = (1/N v \sigma_{\text{gas}})$. Here l is the mean free path, v is the average particle velocity, N is the particle number density, and σ_{gas} is the gas kinetic collision cross section. In air at standard conditions, $l \approx 6 \times 10^{-6}$ cm and $\tau_{\text{trans}} \approx 10^{-10}$ s. Usually the gas kinetic times are short in comparison with the flow times over which appreciable changes in the macroscopic parameters of the gas, density, or energy, take place. When these conditions are satisfied it is possible to assign at every instant of time a "translational" temperature which characterizes the average kinetic energy of translational motion of the particles.

In the past decade, direct integration methods were proposed[2–4] for solving the Boltzmann equation for hard sphere molecules. More recently, Tcheremissine and Agarwal[5] solved the generalized Boltzmann equation using the conservative splitting numerical method for an inert mixture of diatomic gases. In this approach, momentum conservation is given by

$$m^A \xi_i + m^B \xi_i' = m^A \tilde{\xi}_i + m^B \tilde{\xi}_i', \tag{1}$$

where m^A and m^B denote the mass of species A and B, respectively, and ξ_i denotes the component of the particle velocity and the *tilde* quantities denote the postcollision values. The energy conservation is given by

$$\tfrac{1}{2} m^A \xi_i \xi_i + e^A + \tfrac{1}{2} m^B \xi_i' \xi_i' + e^B = \tfrac{1}{2} m^A \tilde{\xi}_i \tilde{\xi}_i + \tilde{e}^A + \tfrac{1}{2} m \tilde{\xi}_i' \tilde{\xi}_i' + \tilde{e}^B, \tag{2}$$

where e^A and e^B are internal energies.

Their study demonstrates that the numerical method of solving the generalized Boltzmann equation is possible, but a careful step-by-step validation is needed to assure accuracy. The work of Tcheremissine[5] outlines the method for the prediction of the macroscopic variables for a Mach 2 shock wave structure consisting of a mixture of two gases. Interestingly, the earlier work of Kosuge *et al.*[2] approximates the collision integrals using the velocity distribution functions at the discrete lattice points in the molecular velocity space. Hence the study was intended to answer the question if their method converged to real collision integrals of the Boltzmann equation. However, the earlier works neither address validation issues of the numerical method nor provide insight into the physical phenomenon. The present study extends a single component Boltzmann flow solver based on the

a)Present Address: School of Aerospace and Mechanical Engineering, University of Oklahoma, Norman, Oklahoma 73019–0601, USA.

method of Tcheremissine[6] to a multispecies Boltzmann solver and characterize a Mach 3 shock wave structure of inert gas mixtures. The paper generalizes the method so that gas mixtures with more than two species can be treated, which has not been done in earlier studies. One of the objectives of the paper is to provide a better physical insight in to the flow physics of shock wave structures.

Previous work by Josyula *et al.*[7] addressed accuracy issues, particularly the requirement of the velocity grid resolution for simulating the internal structure of shock waves in a single component monatomic gas. The direct numerical integration of the Boltzmann equation for the inert gas mixture is a first step toward extending the solution to inelastic and reactive collisions. The present study is generalized for an inert mixture and considers gas mixtures consisting of two and three species to study the nonequilibrium relaxation in the internal structure of the Mach 3 shock wave. It provides physical insight into the observed physical phenomenon relating to the dynamics of the relaxation of the different species in the shock wave structure.

II. DISCRETIZED FORM OF MULTISPECIES BOLTZMANN EQUATION

The Boltzmann equation expresses the behavior of many-particle kinetic system in terms of the evolution of the particle distribution function. The Boltzmann equation is written as

$$\frac{\partial f}{\partial t} + \boldsymbol{\xi}\frac{\partial f}{\partial \mathbf{x}} = I(\boldsymbol{\xi}), \tag{3}$$

where the distribution function, $f\, d\boldsymbol{\xi} d\mathbf{x}$ gives the number of molecules at position $\mathbf{x}$ and velocity $\boldsymbol{\xi}$ at time t. The left hand side of the above equation represents the continuum flow, and the right side denotes the collision term leading to discontinuous jumps in phase space. If the distribution function f is known, the macroscopic variables of the mass, momentum, energy, and stress can be obtained by appropriate weighting and integration.

When considering gas mixtures, inelastic collisions, and reactive energy exchanges, it is convenient to transform the distribution function from velocity ξ_i to momentum p_i^α variables with $p_i^\alpha = m^\alpha \xi_i$ and $f(\boldsymbol{\xi},\mathbf{x},t) \rightarrow f^\alpha(\mathbf{p}^\alpha,\mathbf{x},t)$. Here p_i^A is the initial momentum of species α. Each species, α, in the system is cast on a grid x_i in the configuration space with κ nodes and a uniform three dimensional grid, p_γ^α in momentum space (the subscript γ denotes a momentum node) with N_0 nodes. Thus the system of species Boltzmann equations takes the form

$$\frac{\partial f^\alpha}{\partial t} + \frac{p_i^\alpha}{m^A}\frac{\partial f^\alpha}{\partial x_i} = I^\alpha \quad \text{for species} \quad \alpha = A,B,\ldots. \tag{4}$$

The number of species in the gas mixture is denoted by S. The elastic collision integral for species α takes the form

TABLE I. Rankine–Hugoniot conditions across shock wave for $\gamma = 5/3$.

Mach no. upstream (M_u)	Mach no. downstream (M_d)	p_d/p_u	ρ_d/ρ_u	T_d/T_u
3	0.522	11	3	3.667

$$I^A = \sum_{j=A}^{S}\int_{-\infty}^{+\infty}\int_0^{2\pi}\int_0^{b_m}(\tilde{f}^j\tilde{f}^\alpha - f^j f^\alpha) g_{\alpha j} b db d\varphi d\mathbf{p}^j. \tag{5}$$

Here b_m is the maximum impact parameter with b and φ characterizing the impact for the A-α collision. The relative velocity $\mathbf{g}_{\alpha,j}$ is $\left|\frac{\mathbf{p}^j}{m^j} - \frac{\mathbf{p}^\alpha}{m^\alpha}\right|$. The *tilde* quantities denote the post-collision values.

In the basis of three-dimensional delta functions, the distribution function and the collision integral are represented in the form

$$f^\alpha(\mathbf{p},\mathbf{x},t) = \sum_{\gamma=1}^{N_0} f_\gamma^\alpha(\mathbf{p},\mathbf{x},t)\,\delta(\mathbf{p}-\mathbf{p}_\gamma),$$
$$I^\alpha(\mathbf{p},\mathbf{x},t) = \sum_{\gamma=1}^{N_0} I_\gamma^\alpha(\mathbf{x},t)\,\delta(\mathbf{p}-\mathbf{p}_\gamma). \tag{6}$$

After determining the expansion coefficients for the collision integral in the Eqs. (6), the problem is reduced to solving the coupled system of equations

$$\frac{\partial f_\gamma^\alpha}{\partial t} + \frac{\mathbf{p}_\gamma^\alpha}{m^\alpha}\frac{\partial f_\gamma^\alpha}{\partial \mathbf{x}} = I_\gamma^\alpha \quad \alpha = A,B,\ldots S \quad \gamma = 1,2,\ldots N_0. \tag{7}$$

The conservative numerical method of Tcheremissine,[5] extended to multiple species, is employed. The eight dimensional collision integral is evaluated on a uniform grid following the method of Tcheremissine.[5,6] The discretized collision operator with a symmetry weighting, ϕ_γ^α, is

$$I_\gamma^\alpha = \frac{1}{4}\sum_{j=1}^{S}\sum_{l=1}^{S}\int_\Omega\int_{\varphi=0}^{2\pi}\int_{b=0}^{b_m}\phi_\gamma^\alpha(\tilde{f}^j\tilde{f}^l - f^j f^l) g b db d\varphi d\mathbf{p}^j d\mathbf{p}^l, \tag{8}$$

where

$$\phi_\gamma^\alpha = \delta_{\alpha,l}\delta(\mathbf{p}^l - \mathbf{p}_\gamma^l) + \delta_{\alpha,j}\delta(\mathbf{p}^j - \mathbf{p}_\gamma^j) - \delta_{\alpha,l}\delta(\tilde{\mathbf{p}}^l - \mathbf{p}_\gamma^l) - \delta_{\alpha,j}\delta(\tilde{\mathbf{p}}^j - \mathbf{p}_\gamma^j) \tag{9}$$

and the integration performed over the volume, Ω, in the momentum space. The discretized distribution functions, when weighted by $\Psi = \left(m^\alpha, \frac{p_i^\alpha}{m^\alpha}, \frac{p_i^\alpha p_i^\alpha}{2m^\alpha}\right)$, enable the evaluation of the macroscopic quantities for each species: the mass density ρ, the velocity $\mathbf{u}$, the pressure tensor $\mathbf{P}$, and the heat flux vector $\mathbf{q}$

$$\rho^\alpha = m^\alpha p_0 \sum_\gamma f_\gamma^\alpha, \quad \boldsymbol{u}^\alpha = \frac{m^\alpha p_0}{\rho^\alpha}\sum_\gamma f_\gamma^\alpha \frac{\mathbf{p}_\gamma^\alpha}{m^\alpha}, \tag{10}$$

TABLE II. Two-species inert mixtures of hard sphere gas. [(1) By convention the nominal mass is that of species A and (2) $\chi^{\alpha} \equiv (N^{\alpha}/\Sigma_{j=1}^{S} N^{j})$.]

Case no.	Mass ratio $(m^A:m^B)$	Diameter ratio $(d^A:d^B)$	Concentration ratio $(\chi^A:\chi^B)$
1	2:1	1:1	9:1
2	2:1	1:1	1:1
3	2:1	1:1	1:9
4	4:1	1:1	1:1

$$P_{ij}^{\alpha} = m^{\alpha} p_0 \sum_{\gamma} f_{\gamma}^{\alpha} c_{i,\gamma}^{\alpha} c_{j,\gamma}^{\alpha}, \quad q_i^{\alpha} = \frac{m p_0}{2} \sum_{\gamma} f_{\gamma}^{\alpha} c_{i,\gamma}^{\alpha} (c_{\gamma}^{\alpha})^2,$$

where $p_0 = (\Omega/N_0)$, $c_{\gamma}^{\alpha} = (p_{\gamma}^{\alpha}/m^{\alpha}) - u^{\alpha}$, and $(c_{\gamma}^{\alpha})^2 = (c_{1,\gamma}^{\alpha})^2 + (c_{2,\gamma}^{\alpha})^2 + (c_{3,\gamma}^{\alpha})^2$ In the above equation, c denotes the peculiar velocity, u the macroscopic velocity in the direction parallel to the flow, and ρ is the macroscopic mass density.

The steady flow is treated as one-dimensional in the configuration space and three dimensional in momentum space. A uniform equilibrium state is assumed far upstream and downstream of a standing normal shock wave. Number conservation, conservation of total momentum, and conservation of total energy lead to a generalized set of Rankine–Hugoniot relations.[2] See Table I. The distribution function boundary conditions up and downstream were specified by a drifting Maxwellian. At upstream $-\infty$

$$f_u^{\alpha}(\mathbf{p},\mathbf{x},t) = N_u^{\alpha}(x)(2\pi m^{\alpha} k T_u)^{-3/2} \times \exp\left\{ - \frac{[(p_x^{\alpha} - \bar{p}_u^{\alpha})^2 + p_y^{\alpha 2} + p_z^{\alpha 2}]}{2 m^{\alpha} k T_u} \right\}. \quad (11)$$

At downstream ∞

$$f_d^{\alpha}(\mathbf{p},\mathbf{x},t) = N_d^{\alpha}(x)(2\pi m^{\alpha} k T_d)^{-3/2} \times \exp\left\{ - \frac{[(p_x^{\alpha} - \bar{p}_d^{\alpha})^2 + p_y^{\alpha 2} + p_z^{\alpha 2}]}{2 m^{\alpha} k T_d} \right\}, \quad (12)$$

where $\bar{p}_u^{\alpha}$ and $\bar{p}_d^{\alpha}$ denote the average upstream and downstream momenta in the flow direction.

III. RESULTS AND DISCUSSIONS

The shock wave structure in a two- and three-species gas mixture of inert gases was analyzed for a variety of mass ratios and molecular diameters in the hard sphere collision approximation. Validation results are presented initially for the multispecies solver. The results are then discussed for the cases shown in Tables II and III.

TABLE III. Three-species inert mixtures of hard sphere gas. [(1) By convention the nominal mass is that of species A and (2) $\chi^{\alpha} \equiv (N^{\alpha}/\Sigma_{j=1}^{S} N_j)$.]

Case no.	$m^A:m^B:m^C$	$d^A:d^B:d^C$	$\chi^A:\chi^B:\chi^C$
5	1:0.9:0.8	1:1:1	1:2:3

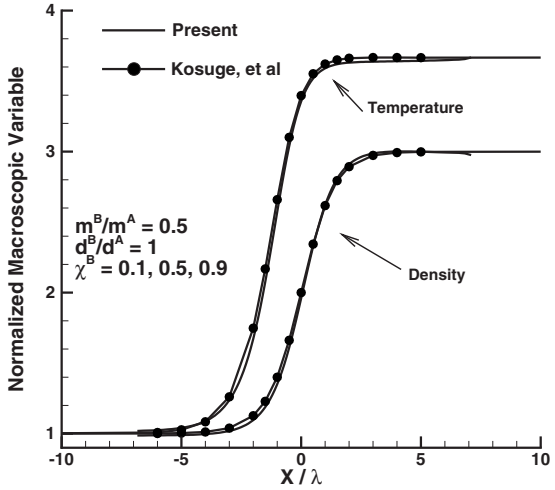

FIG. 1. Code verification: comparison of macroscopic density and temperature for mass ratio of 0.5, diameter ratio of 1, and concentration of B of 0.1, 0.5, and 0.9 with Kosuge *et al.* (Ref. 2) in the Mach 3 shock wave structure.

A. Verification of Boltzmann equation solver for inert gas mixture

The initial verification of the multispecies Boltzmann equation solver consists of comparing the macroscopic parameters and distributions function for the two monatomic species A and B with equal concentrations, and the same mass and hard sphere diameter ratio. Results from the single component Boltzmann equation solver[7] matched within machine accuracy those of multicomponent Boltzmann equation solver for identical gas properties. Further, the macroscopic parameters and velocity distribution function were within machine accuracy for the species A and B.

Figures 1 and 2 show comparison of density, streamwise velocity, and temperature (normalized by their upstream values) for $\chi^B = 0.1, 0.5, 0.9$ with computations of Kosuge *et al.*[2] The comparison of macroscopic variables of density, velocity, and temperature of the total mixture between the two solvers show excellent agreement.

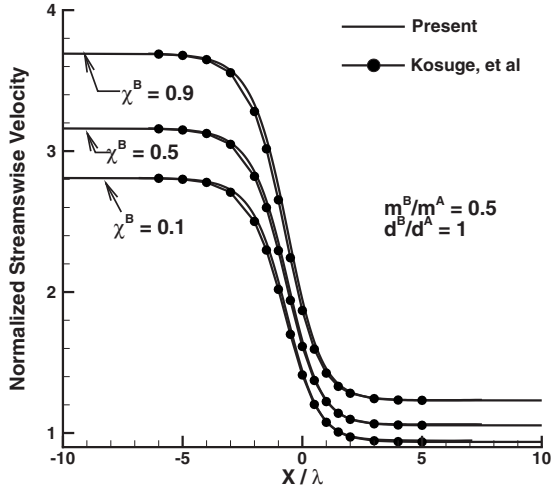

FIG. 2. Code verification: comparison of macroscopic streamwise velocity for mass ratio of 0.5, diameter ratio of 1, and concentration of B of 0.1, 0.5, and 0.9 with Kosuge, *et al.* (Ref. 2) in the Mach 3 shock wave structure.

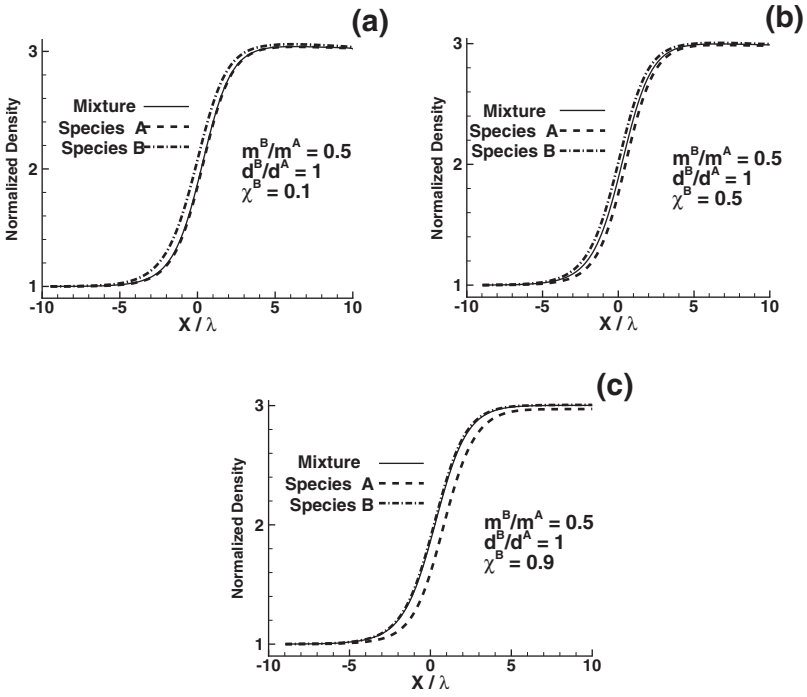

FIG. 3. Density distribution in a Mach 3 shock wave with hard sphere collision model for mass ratio of 0.5, diameter ratio of 1, and concentration as (a) χ^B=0.1, (b) χ^B=0.5, and (c) χ^B=0.9.

B. Two-species mixture with varying concentration ratio and mass ratio

1. Effect of varying species concentration

Figure 3 shows the individual species' densities and mixture density in the Mach 3 shock wave structure for mass ratio of 0.5, diameter ratio of 1, and for different concentrations of species B, as shown in the Table II. The density is normalized with its upstream value. For all concentrations considered, χ^B=0.1, 0.5, and 0.9 [Figs. 3(a)–3(c)] the lighter component (species B) transitions earlier from its undisturbed upstream condition to the shock and maintains a slightly higher density than the heavier component throughout the shock wave.

The streamwise velocity component is shown for the Mach 3 shock wave in Fig. 4 for different concentrations of B(χ^B) of 0.1, 0.5, and 0.9 for mass ratio of 0.5, diameter ratio of 1. The velocity of the lighter component, species B, transitions earlier from its undisturbed free-stream value to the shock wave for all concentrations considered.

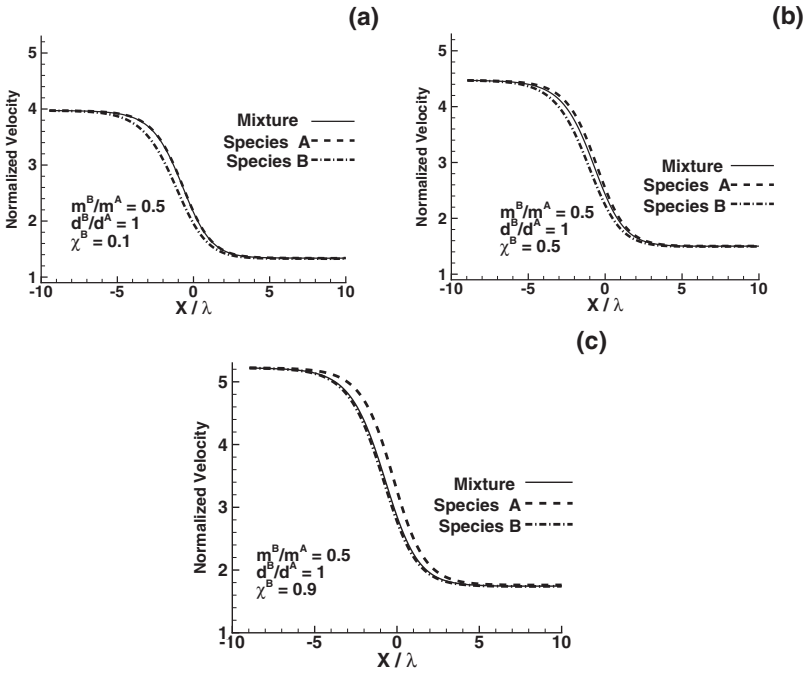

FIG. 4. Streamwise velocity distribution in a Mach 3 shock wave with hard sphere collision model for mass ratio of 0.5, diameter ratio of 1, and concentration as (a) χ^B=0.1, (b) χ^B=0.5, and (c) χ^B=0.9. Normalized velocity=$u/(2kT_u/m^A)^{1/2}$.

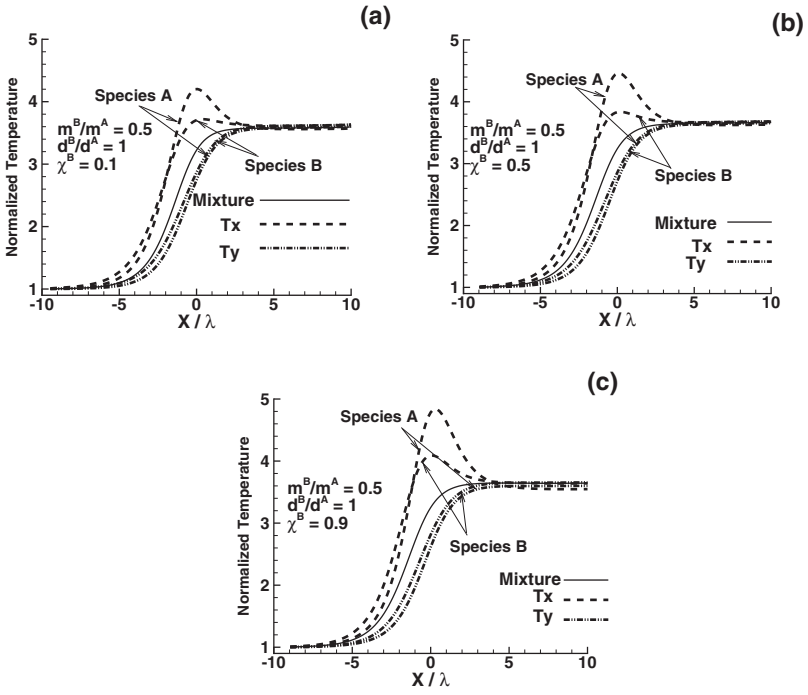

FIG. 5. Temperature distribution in a Mach 3 shock wave with hard sphere collision model for mass ratio of 0.5, diameter ratio of 1, and concentration as (a) χ^B=0.1, (b) χ^B=0.5, and (c) χ^B=0.9.

The magnitude and trends of velocity and density profiles in the shock wave noted above (Fig. 3 and 4) are evidences of conservation of mass flux in the different gas mixtures. In summary, for a gas mixture with fixed values of mass ratio and diameter ratio, the concentration ratio has very little effect on mixture density, velocity, and temperature. There is, however, an effect of varying the concentration on the individual temperatures, as well as the component temperatures: Tx and Ty (discussed next).

Figure 5 shows parallel and perpendicular components of temperature and the mixture temperature for the three concentrations, χ^B=0.1, 0.5, and 0.9 for mass ratio of 0.5, and diameter ratio of 1. The parallel (Tx) and perpendicular (Ty) components of the temperature are calculated from their corresponding pressure components

$$kTx = m\overline{u'^2} = p_{xx}/n, \tag{13}$$

$$kTy = m\overline{u}'^2 = p_{yy}/n. \tag{14}$$

For all three concentrations, there is overshoot of parallel component (Tx) for both the heavier (species A) and lighter species of the gas mixture. The Tx component of the heavier particle (species A) has a greater magnitude and overshoot than that of species B. It is also noted that the greater the value of χ^B, the higher the overshoot of the Tx for both the heavier species (species A) and lighter species.

2. Overshoot of parallel component of temperature

Figure 6 depicts the parallel and perpendicular components of the momentum distribution function for the binary gas mixture (species A and B) for χ^B=0.1 for mass ratio of

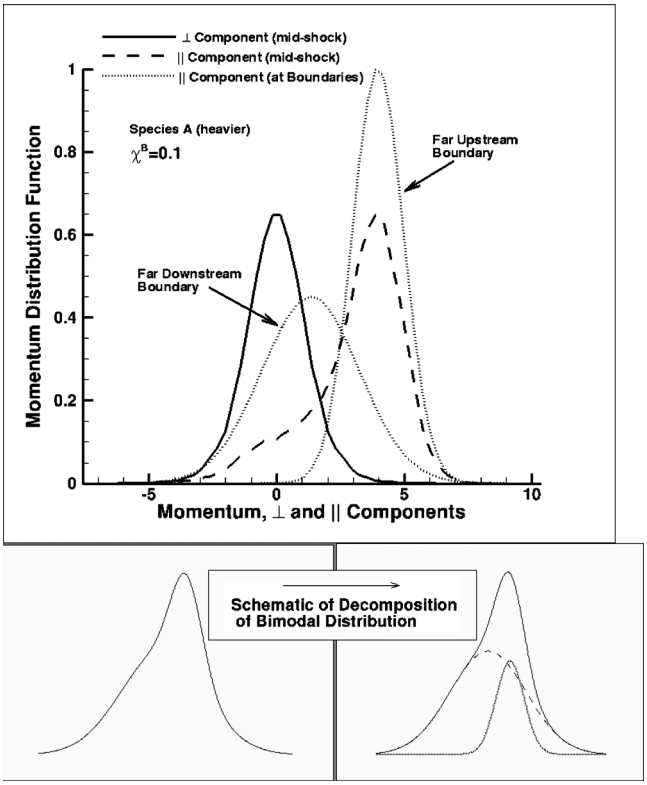

FIG. 6. Components of momentum distribution function in a Mach 3 shock wave with hard sphere collision model for mass ratio of 0.5, diameter ratio of 1, χ^B=0.1, for species A (heavier). Schematic shown in the bottom gives the decomposition of the bimodal distribution into two Maxwellian distributions giving insight to the parallel temperature overshoot.

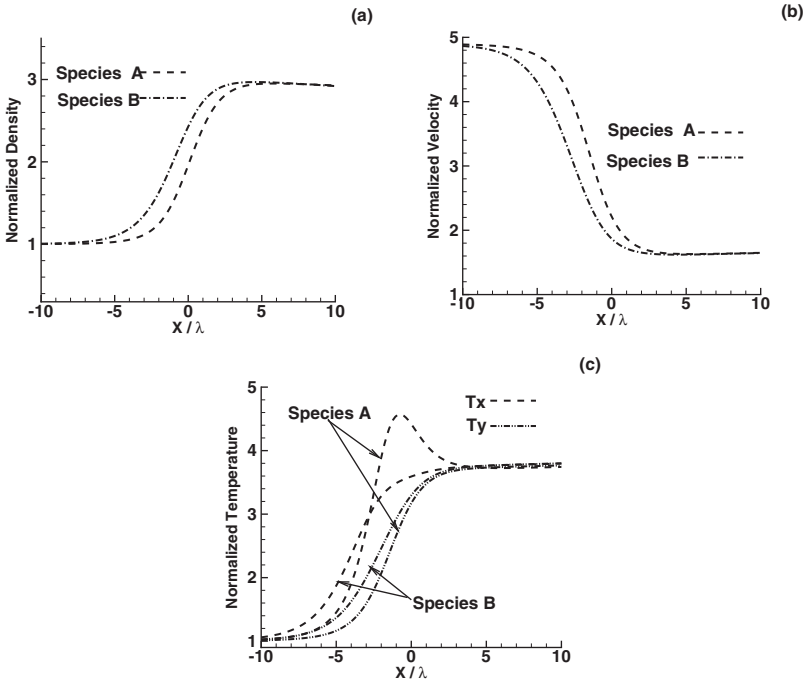

FIG. 7. Density, velocity, and temperature distribution in a Mach 3 shock wave with hard sphere collision model for mass ratio of 0.25, diameter ratio of 1, and concentration of B of 0.5, (a) density, (b) streamwise velocity, and (c) temperature.

0.5, and diameter ratio of 1. Species A is the heavier component and Species B the lighter. Comparisons of results of the species A and species B show that the momentum distribution function of the parallel component is bimodal, which can be related to the temperature overshoot for the *Tx* component seen in the preceding figure (Fig. 5). The schematic shows the decomposition of the bimodal distribution into two distinct Maxwellian distributions, one corresponding to the wide part of the bimodal, which contributes to the parallel temperature overshoot. The parallel temperature *Tx* is given by

$$\frac{kT_x}{m} = \nu_A \frac{kT_A}{m} + (1-\nu_A)\frac{kT_B}{m} + \nu_A(1-\nu_A)[\langle v_A\rangle - \langle v_B\rangle]^2, \tag{15}$$

where $\nu_A = [N_A/(N_A+N_B)]$, $\nu_B = [N_B/(N_A+N_B)]$, $\langle v_A\rangle$ and $\langle v_B\rangle$ denote the average velocities of species A and B, respectively.

3. Effect of lowering the mass ratio, m^B/m^A, from 0.5 to 0.25

Figure 7 shows the macroscopic density, streamwise velocity, and temperatures for species A and B inside the Mach 3 shock wave structure for mass ratio of 0.25, diameter ratio of 1, and for concentration of B(χ^B) of 0.5. When the mass ratio (m^B/m^A) is lowered to 0.25 (Fig. 7), the trends of macroscopic parameters for $m^B/m^A=0.25$ are similar to those of $m^B/m^A=0.5$ [Figs. 3(b), 4(c), and 5(b)]. However, lowering the mass ratio shows an increase in shock wave thickness and a greater disparity of the macroscopic density and velocity in the two species, further evidenced in the behavior of the distribution function, discussed next. The lowering of the mass ratio shows a very small difference in the downstream boundary values in the profiles of the temperature components. This difference is due to the difficulty in satisfying the phase space grid requirements for gas mixtures of widely different masses. It is noted that in the present numerical method, a single momentum grid is used for the two masses with the mass ratio of 0.25; this issue is related to the higher demand placed on the phase space grids for satisfying the resolution requirements of both the masses. This numerical issue is further discussed in a subsequent section in Fig. 10.

4. Velocity distribution functions for two different mass ratios

The velocity distribution function is shown for two different mass ratios (m^B/m^A of 0.5 and 0.25) in the shock wave in Figs. 8 and 9. The diameter ratios ($d^B/d^A=1$) and concentrations ($\chi^B=0.5$) are kept fixed in both cases. The panels (a) and (d) are at the $-\infty$ and $+\infty$ locations set to Maxwellian distribution function boundary conditions given by the Rankine–Hugoniot relations for a Mach 3 shock wave. The panels (b) and (c) are located inside the shock wave, at $X/\lambda=-0.4$ and +2, respectively. For both Figs. 8 and 9, the results for the species A are presented at the top and species B at the bottom of the figure.

Figure 8 shows the velocity distribution function for a $m^B/m^A=0.5$, diameter ratio of 1, and concentration of species B of 0.5. The distribution functions at all X/λ locations are normalized to the peak value at the far upstream location. For both species, at the far upstream and downstream locations of $-\infty$ and $+\infty$, the boundary conditions are the Maxwellian distribution functions. Inside the shock structure, Figs. 8(b) and 8(c), the distribution functions are non-

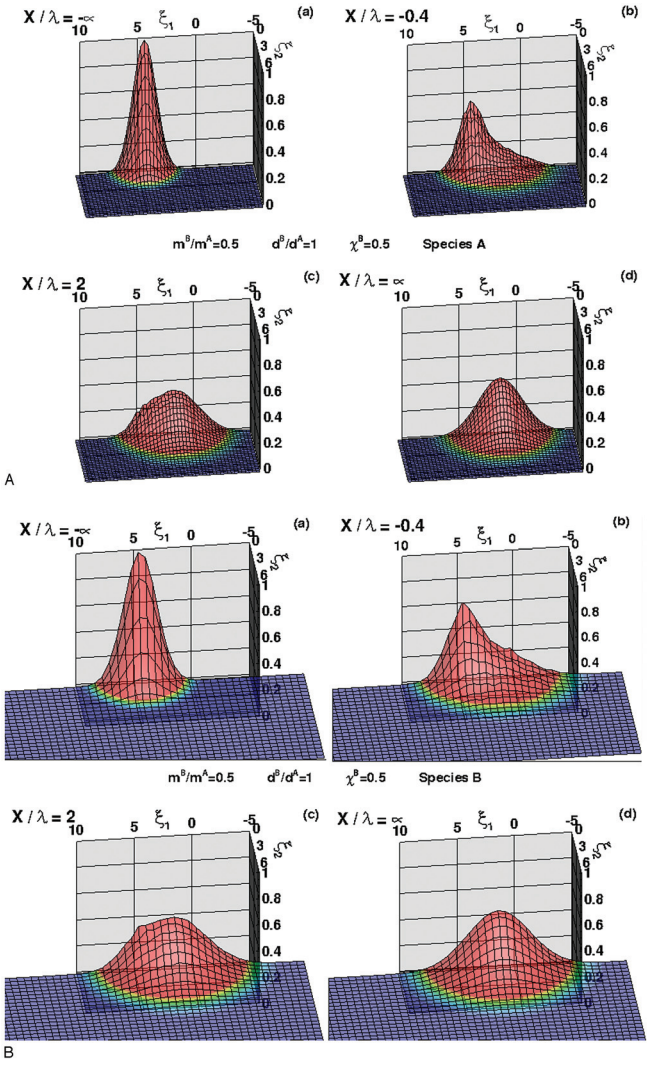

FIG. 8. (Color) Velocity distribution function inside a Mach 3 shock wave with hard sphere collision model for mass ratio of 0.5, diameter ratio of 1, and concentration of B of 0.5, species A (top), species B (bottom), (a) $x/\lambda=-\infty$, (b) $x/\lambda=-0.4$, (c) $x/\lambda=2$, and (d) $x/\lambda=\infty$.

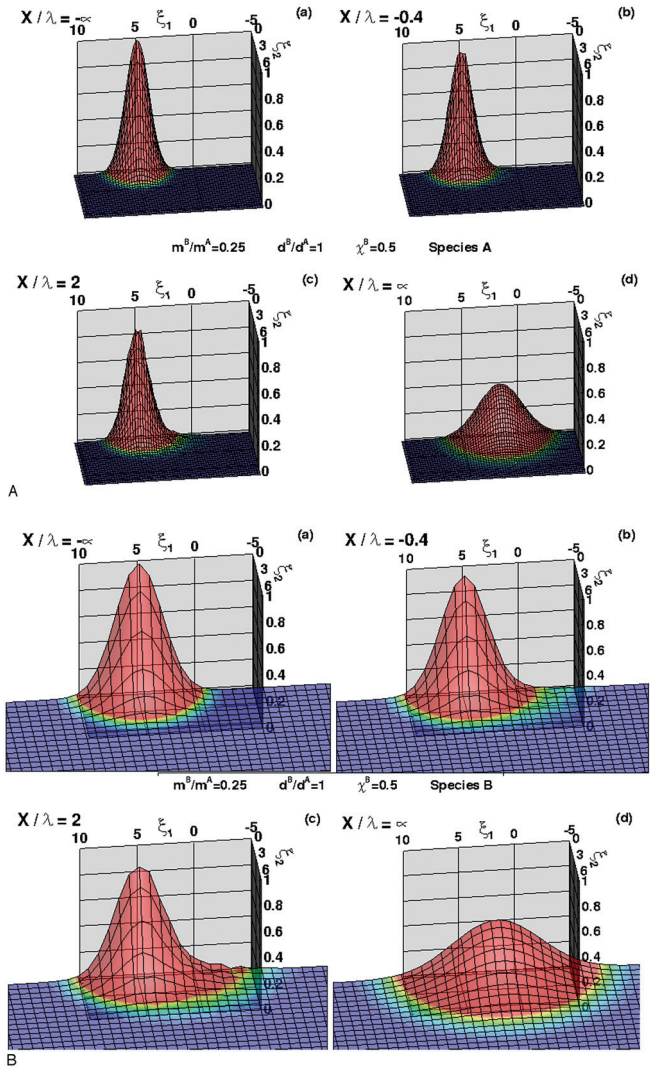

FIG. 9. (Color) Velocity distribution function inside a Mach 3 shock wave with hard sphere collision model for mass ratio of 0.25, diameter ratio of 1, and concentration of B of 0.5, species A (top), species B (bottom), (a) $x/\lambda=-\infty$, (b) $x/\lambda=-0.4$, (c) $x/\lambda=2$, and (d) $x/\lambda=\infty$.

Maxwellian, and are slightly wider for the lighter species B (see bottom set of figures) than those of species A (see top set of figures).

Figure 9 shows the effect of lowering the mass ratio ($m^B/m^A=0.25$) on the velocity distribution functions. The distribution functions of species A (heavier species) for both mass ratios (top set in Figs. 8 and 9) have a small variation in their respective widths. However, one can see a larger width of the distribution function for species B (lighter species) for the lower mass ratio of 0.25 at all the locations in the shock structure (bottom set in Figs. 8 and 9).

C. Effect of momentum grid resolution for different mass ratios

The multispecies Boltzmann equation was solved in momentum space in the present work, where the shared, single momentum grid has to satisfy the momentum resolution for both the species. Here, the effect of momentum grid resolution is presented for each species for differing mass ratios to show the relative differences. The effect of momentum grid resolution for each species A and B for differing mass ratios of 0.5 and 0.25 is shown at the far upstream location of $-\infty$ and far downstream location of $+\infty$ in Fig. 10. The momentum grid was held constant at $36\times18\times18$ points in the phase space for both cases. The upstream and downstream boundaries are set as Maxwellian distribution functions for the conditions given by the Rankine–Hugoniot relations for the Mach 3 shock wave. The momentum distribution function for the lighter component (species B) has a smaller width than species A at $-\infty$ and $+\infty$. On examining the number of grid points defining the upstream Maxwellians for species B, it is seen that while 14 points [Fig. 10(a)] define the upstream distribution function for mass ratio of 0.5, only nine points [Fig. 10(b)] define the upstream distribution function for mass ratio of 0.25. The numerical problems seen in temperature predictions at the downstream boundary for the lower mass ratio of 0.25 [shown earlier in

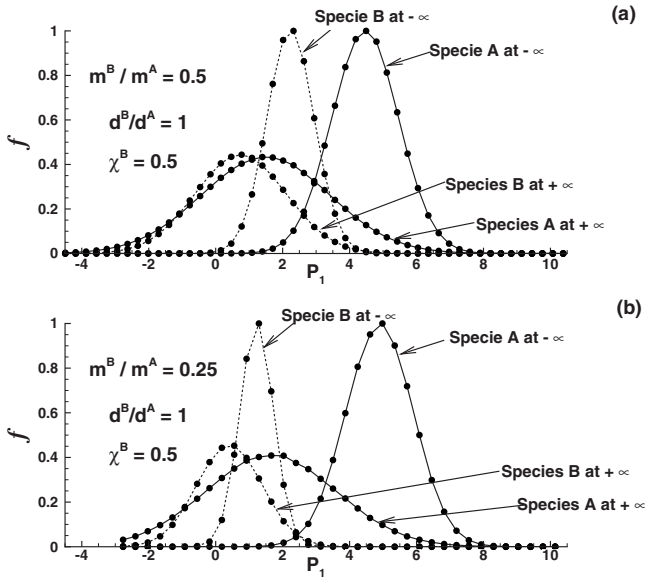

FIG. 10. Effect of momentum grid resolution in a Mach 3 shock wave of two-species gas mixture with hard sphere collision model with $36\times18\times18$ points in phase space for diameter ratio of 1 and concentration of B of 0.5, (a) $m^B/m^A=0.5$, and (b) $m^B/m^A=0.25$.

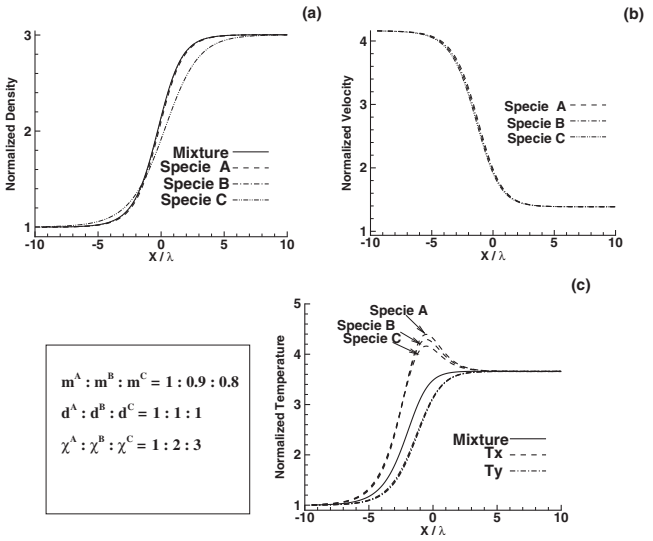

FIG. 11. Density, velocity, and temperature distribution in a Mach 3 shock wave with hard sphere collision model for a three-species gas mixture.

Fig. 7(c)] may be attributed to the lack of proper momentum grid resolution for the lighter species B. It may be concluded that the more demanding momentum grid requirements for individual
species with smaller widths of the distribution function are an important consideration in sizing the phase space grids for solving the multispecies Boltzmann equation for gas mixtures.

D. Three-species gas mixture

Results for a three-species gas mixture are presented for differing mass ratios, with the same hard sphere diameters, and variation in concentration ratios for the three species. Figure 11 shows the density, velocity, and temperature distributions for the individual species A, B, and C as well as the mixtures in a Mach 3 shock wave structure with the following ratios: $m^A:m^B:m^C=1:0.9:0.8$, $d^A:d^B:d^C=1:1:1$, and $\chi^A:\chi^B:\chi^C=1:2:3$. Figure 11(a) shows that the density variation for species A, B and C is close to each other as well as the mixture. The velocity, Fig. 11(b), shows very little variation between the three species as well, confirming that the mass flux is conserved. The temperature variation, Fig. 11(c), shows that the parallel component (Tx) for species A has the greatest overshoot, followed by B and then C near $X/\lambda=-0.1$. At all other X/λ locations in the shock wave, the Tx component temperature profiles for the three species show little variation with each other. The perpendicular components (Ty) for the three species show little variation throughout the shock wave.

Figure 12 shows the velocity distribution function for the three species A, B, and C at different locations in the shock wave. At locations inside the shock wave, $X/\lambda=-0.4$ and $X/\lambda=+2$, one can see the non-Maxwellian distribution function. It is noted that for the three-species gas mixture with small variation in mass ratio and identical diameter ratio, the distribution function is proportional to the concentration ratio.

IV. CONCLUDING REMARKS

A numerical study was performed for the solution of the internal structure of shock waves in monatomic gas mixtures, assuming the hard sphere collision model. The multispecies Boltzmann equation was solved by the conservative discrete ordinate method of Tcheremissine. Macroscopic parameters predicted in the present study for Mach 3 shock wave agree well with those from the previous work of Kosuge, Aoki, and Takata. The effect of species concentration and mass ratio in the shock wave was presented by macroscopic variables and distribution functions.

For a two-species gas mixture, fixed mass ratio of 0.5, and diameter ratio of 1, the concentration of the lighter species was varied as 0.1, 0.5, and 0.9. The mixture density, velocity, and temperature were found to be relatively insensitive to the change in concentration. For all concentrations, the macroscopic variables of the light component start to transition from the upstream freestream value earlier than the corresponding variables of heavy component. The macroscopic density and velocity of the light component reach the downstream asymptotic values earlier than the heavy component. The macroscopic density, velocity, and temperature of the mixture are very close to the values of the heavy component when the concentration of the heavy component is large. The temperature overshoot of the parallel component near the center of the shock wave is highest for the heavy component when the concentration of the heavy component is the smallest. The relative comparison of the parallel and perpendicular components of momenta show that that the parallel component has a wider distribution, which has the temperature overshoot. The relative magnitudes of the parallel temperature overshoots for different mixture concen-

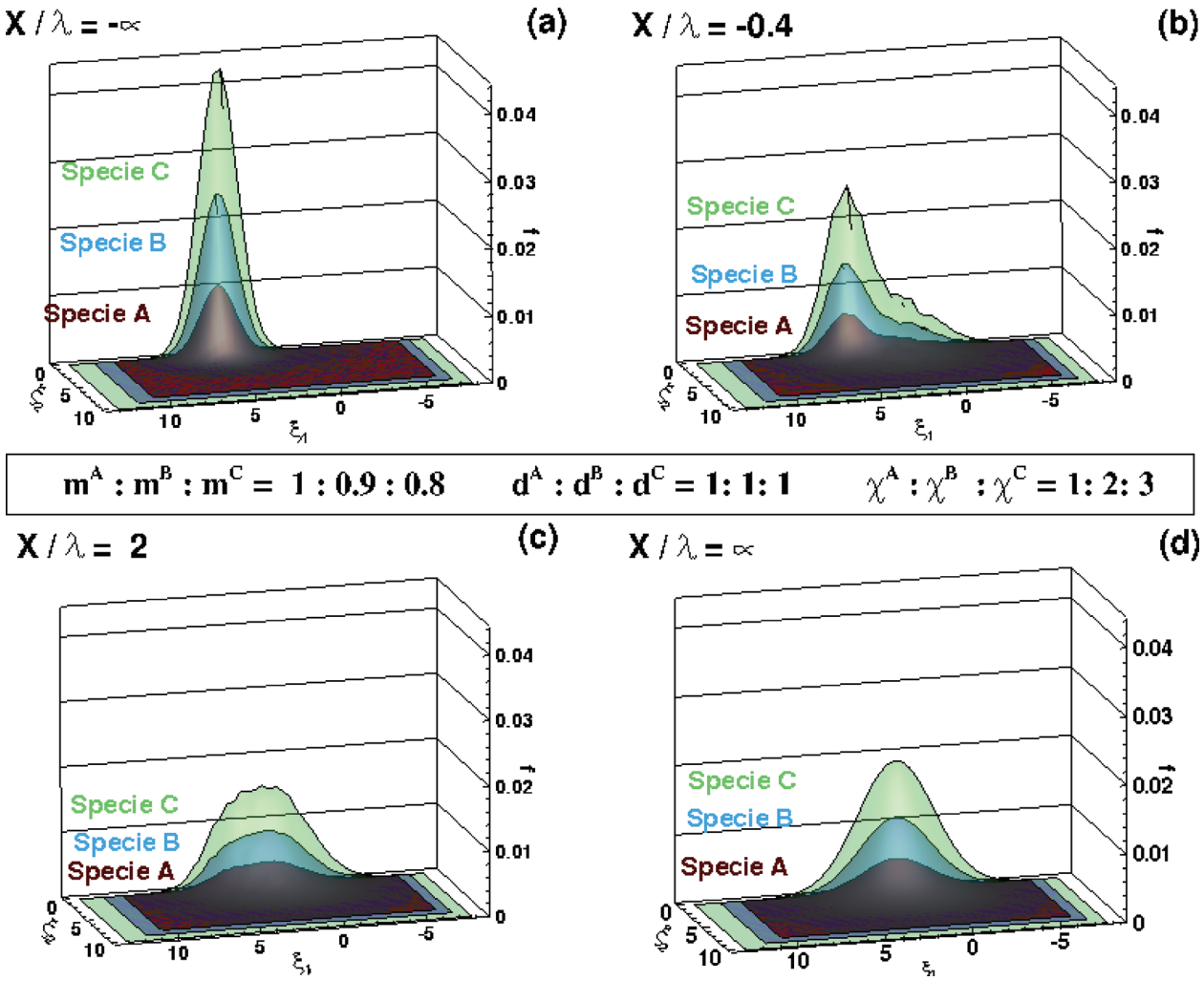

FIG. 12. (Color) Velocity distribution function inside a Mach 3 shock wave with hard sphere collision model, (a) $x/\lambda=-\infty$, (b) $x/\lambda=-4$, (c) $x/\lambda=2$, and (d) $x/\lambda=\infty$.

trations corresponds with the relative magnitudes of the parallel components of momenta.

For a binary gas mixture, fixed diameter ratio of 1, and fixed concentration of the lighter species of 0.5, two mass ratios were considered: 0.5 and 0.25. There was a greater shock thickness with the lowering of the mass ratio. The momentum grid resolution for the lighter component was more demanding for the lower mass ratio.

For a three-species gas mixture, with the mass ratio of 1:0.9:0.8, diameter ratio of 1:1:1, and concentration ratio of 1:2:3, there was little variation of densities and velocities between the three species across the shock wave. The overshoot of the parallel temperature component of the heaviest species was noted to be the highest and occurred near the middle of the shock wave. The behavior of the distribution function was found to be consistent with the underlying physics and complemented the prediction of the macroscopic variables for all the cases considered in this study.

ACKNOWLEDGMENTS

Support is provided by U.S. Air Force Office of Scientific Research contract monitored by F. Fahroo.

[1]S. G. Labbe, S. Perez, S. Fitzgerald, J. M. A. Longo, R. Molina, and M. Rapuc, "X-38 integrated aero- and aerothermodynamic activities," Aerosp. Sci. Technol. **3**, 485 (1999).
[2]S. Kosuge, K. Aoki, and S. Takata, "Shock-wave structure for a binary gas mixture: Finite-difference analysis of the Boltzmann equation for hard sphere molecules," Eur. J. Mech. B/Fluids **20**, 87 (2001).
[3]T. Ohwada, "Structure of normal shock waves: Direct numerical analysis of the Boltzmann equation for hard sphere molecules," Phys. Fluids A **5**, 217 (1993).
[4]A. Raines, "Study of a shock wave structure in gas mixtures on the basis of the Boltzmann equation," Eur. J. Mech. B/Fluids **21**, 599 (2002).
[5]F. G. Tcheremissine and R. K. Agarwal. "A conservative numerical method for solving the generalized Boltzmann equation for an inert mixture of diatomic gases," AIAA Paper No. 2009-1581, 2009.
[6]F. G. Tcheremissine, "Solution of the Boltzmann kinetic equation for high-speed flows," Comput. Math. Math. Phys. **46**, 315 (2006).
[7]E. Josyula, K. Xu, C. Suchyta, and W. F. Bailey, "Kinetic methods for solving the internal structure of shock waves," AIAA Paper No. 2009-3841, 2009.